Malaysian NANO-An International Journal

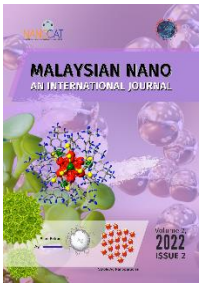

Research article

Received September 10, 2022
Revised October 6, 2022
Accepted October 14, 2022

DOI:
https://doi.org/10.22452/mnij.vol2no2.1

Corresponding authors:
faysalkabir.dup@gmail.com

Tailoring the size and magnetic property of biogenic silver nanoparticles

S.M. Rayhan[a], M.F. Kabir[b*], J. Ferdousy[c], A. K. M. Atique Ullah[d], M. M. Rahman[a]

[a] Dept. of Physics, University of Dhaka, Dhaka-1000, Bangladesh,
[b]Health Physics Division, Atomic Energy Centre, Bangladesh Atomic Energy Commission, Dhaka-1000, Bangladesh
[c] Dept. of EEE, Green University of Bangladesh, Dhaka-1207, Bangladesh
[d]Chemistry Division, Atomic Energy Centre, Bangladesh Atomic Energy Commission, Dhaka-1000, Bangladesh

Abstract

By exploring biological sources, the area of nanotechnology is currently thriving and offers a fresh method. Plant extract-mediated green nanomaterial synthesis has gained appeal as a result of its cost-effectiveness and environmentally beneficial characteristics. In this study, Ag NPs were successfully synthesized from reducing Ag+ ions using *Mangifera indica* leaf extracts as a source of reducing and capping agents. Several different microscopic and spectroscopic approaches were used in order to characterize the produced Ag NPs. Analyses using XRD and SEM have been carried out to look into the morphology of the generated Ag NPs. The (XRD) pattern peaks are associated with the metallic silver in the (FCC) shape. Silver nanoparticles average grain size is in the 10–100 nm range for all concentrations of $AgNO_3$. The shape of the produced silver nanoparticles was determined to be round and spherical by (SEM), and their total size was determined to be between 50 and 100 nm. Analysis using EDX spectroscopy also demonstrated the production of silver and the presence of components that performed the function of a capping agent. (FT-IR) spectra were performed in order to determine the organic groups like carbonyl, hydroxyl, amine, and protein molecules. Analysis using (FT-IR) spectroscopy publicized the presence of flavonoids, polyphenols, and amide groups, all of which are candidates for being responsible for the environmentally friendly creation of silver nanoparticles. From (VSM) analysis, the biosynthesized Ag NPs were weak ferromagnetic in nature, which would be a potential research arena, especially for device application and medical equipment construction using these magnetic crystalline AgNPs.

Keywords: Ag NPs, synthesized, X-ray Diffraction, TGA, magnetization

1. Introduction

In recent years, nanotechnology has exhibited quick and successful growth since it enables the development of known materials with diverse characteristics [1]. Any material's inherent qualities may be altered by shrinking it to the nanoscale [2]. As a result, the characteristics of a nano structured material might be vastly different from those of the bulk material, allowing it to be used in various applications [3]. Nanoparticles made of metal have a large surface area in addition to a high surface atom fraction [4]. As a result of the singular physicochemical features that nanoparticles possess including even enzymatic performance, optical characteristics, electrical characteristics, magnetic properties, and antibiotic capabilities, nanoparticles are becoming an increasingly important component [5]. Because of their unique approaches to synthesis, scientists are becoming more interested in them. Over the previous several years, the combination of metal nanoparticles has been an essential topic of research in modern material science [6]. In high-sensitivity intramolecular surveillance, diagnostics, therapies, catalyst supports, and microelectronics, silver particles have significant potential [7]. There is, however, still a need for environmentally viable and friendly products [8]. It is general knowledge that silver has an impact that is inhibitory on a wide variety of bacterial strains and germs that are often found in industrial and medicinal procedures [9].The use of silver and nanoparticles made of silver have a diverse array of applications in the realm of therapeutics, including antimicrobial silver ointments and lotions for the skin, which are used to treat burns and open wounds without the risk of infection [10]. Silver-impregnated polymers are used in the manufacture of medical equipment and implants, among other things [11]. Silver-embedded textiles are now being used in the sports goods sector of the textile industry [11]. Nanoparticles are able to be manufactured by a variety of chemical, physical, and biological processes [12]. Nevertheless, chemical and physical methods produce toxic products and lead to non-eco-friendly and hazardous conditions; moreover, the precise control plans are costly [13].

Stabilize metal nanoparticles with regulated size and shape; there has been a quest for an economical, safe, and dependable non-toxic and "green" approach; the revolutionary process of so-called green synthesis is an example of one such approach. A "green synthesis" of nanoparticles is one that employs chemicals that are safe, non-toxic, and beneficial to the environment. Plants provide a superior platform for green synthesis due to the absence of potentially harmful compounds on their surfaces, as well as the presence of naturally occurring capping agents [14]. Moreover, the use of plant extracts also decreases the cost of the plant extracts themselves.

There have already been several trials like this one started, including synthesizing a wide variety of metal nanoparticles produced by employing fungi such as *Fusarium oxysporum* and *Penicillium sp*., in addition to using certain bacteria such as *Bacillus subtilize* [15]. This method also has the advantage of having a particular benefit, which is that the plants can be found in a wide variety of locations, are easily accessible, are significantly less dangerous to work with, and assist as a source of numerous different metabolites [16]. In the process of creating nanoparticles, leaf broths, the green parts of plants, and all other kinds of herbs are also used as an alternative to hazardous chemicals [17].

The flourishing "Green synthesis" has the potential to become a viable alternative to the traditional chemical production of nanoparticles. Thus, scientists worldwide have been searching for new substrates from nature. However, no report is available on Ag NPs synthesis using several concentrations of $AgNo_3$ solution and mango *(Mangifera indica*) leaf extract to the best of our knowledge. *Mangifera indica* is the most common favourite food in our country. Additionally, it has antioxidant, hypertensive, and anti-diabetic actions are some other beneficial effects[18].

As a result, the extract of the leaves of *Mangifera indica* might be a possible option for use in the green production of silver nanoparticles as a source of reducing as well as capping agents. The nuclei of silver should be as tiny as possible for maximum antibacterial action [18]. Aside from that, the catalytic activity of nanoparticles is reliant on their size, structure, shape, and the chemical-physical environment in which they are put. [19]. Changing the synthesis processes and adding reducing agents and stabilizers are often used to precisely control form, size, and size distribution.

2. Materials and Methods

2.1. Chemicals and reagents: $AgNO_3$ (Merck, Germany), *Mangifera indica* (mango) tree leaves, and deionized water.

2.2. Preparation of Mangifera indica (Mango) leaf extract

One of the most well-known and often used expressions in all tropical fruits is the mango. It is found almost everywhere globally. We collected fresh mango leaves locally, washed them to remove the impurities multiple times with fresh water, then sun-dried them to eliminate any remaining moisture after that blinded them for making powder (Figure 1). After that, the plant extract was made by combining 5 grams of the powdered leaf with 1 liter of deionized water in a conical flask and then heating the mixture to 80 degrees Celsius for ten minutes. After filtering the Leaf extract solution was preserved at 4°C in the refrigerator.

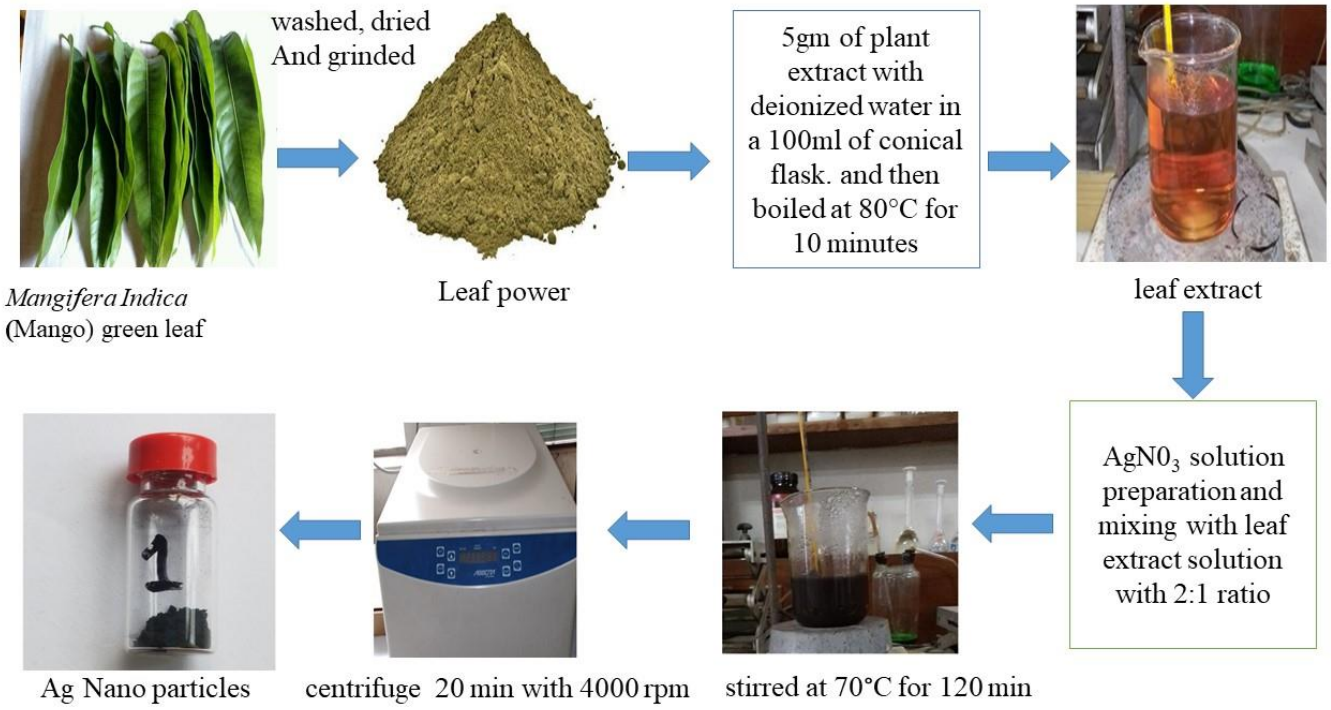

Figure 1: Schematic diagram of the synthesis of Ag NPs

2.3. Synthesis of silver nanoparticles

A total of 300 mL of 20 mM$AgNO_3$ solution was added to 150 ml of leaf extracts at a ratio of 2:1 (Figure 1). The solution was then hand-shaken to ensure thorough mixing. After that, the solution was agitated with a magnetic string at a temperature of 70 degrees Celsius for an hour and a half. The reaction was allowed to settle at room temperature. Then it was subjected to a centrifuge for 20 min at room temperature with 4000 rpm. The supernatant was separated. The same procedure was repeated for 50 mM $AgNO_3$ and 100 mM$AgNO_3$.

2.4. Energy Dispersive X-ray (EDX) Spectra and Scanning Electron Microscopy (SEM) analysis

JEOL, JSM 7600 F, in Japan, carried out the EDX investigation employing a voltage of 15 kV for the acceleration and a current of 12 mA for the emission. SEM was performed by JEOL, using their model JSM 7600 F from Japan. An acceleration voltage of 15 kV was used, and a 12 mA emission current was measured. EDX spectra performed the elemental analysis of the synthesized silver nanomaterial. The dried powdered Ag nanomaterial was positioned on a 1 cm × 1 cm conducting steel plate. After that, the steel plate was situated above a conductive carbon strip that had been bonded. Furthermore, the sample was positioned inside the primary SEM chamber that was connected to the EDX apparatus.

2.5. Infrared spectra analysis

FT-IR spectra were collected using a JASCO-FTIR-6300 from Japan, and wave numbers ranging from 400 to 4000 cm^{-1} were used for the collection. In this particular instance, samples with a weight-to-volume ratio of one percent (w/w) were combined with KBr powder and formed into a thin slice. The infrared spectrum of the dried samples of mango leaf to powder and synthesized silver nanomaterial were recorded on an FTIR spectrometer in 4000 – 400 cm^{-1}. It is usual practice to produce IR spectra of solid samples by combining a little amount of the substance to be tested with crystals of dry and pure KBr, then mixing and grinding the mixture. A pestle was used inside of a mortar to achieve the task of crushing the components and mixing them together. Following this step, the powder mixture was put into a metal container and then exposed to between 8 and 10 tons of pressure in order to form a pellet. Following that, the pellet was positioned in such a way that it would be lighted by the IR beam in order to facilitate the taking of measurements.

2.6. Thermo-gravimetric analysis (TGA)

TGA was performed in an environment containing N_2 using the TGA instrument SDR Q-600, which was set to operate from 25 to 800 degrees Celsius with a heating rate of 10 degrees Celsius per minute. This investigation is being carried out to find out how temperature affects phase transition. The silver nanoparticles were heat-treated at 100 °C, 200 °C, 300 °C, 400 °C, 500 °C, 600 °C, 700 °C, and 800 °C for three hours in a muffle furnace.

2.7. Procedure for X-ray diffraction

An XRD investigation was carried out with the assistance of a Philips PANalytical X'PERT PRO X-ray powder diffractometer that was fitted with CuKa radiation (1.5418 A). The voltage was 40 keV, and the current was 30 mA, while the spectra to detect were being recorded. Powdered silver (Ag) nanoparticles were subjected to X-ray diffraction analysis in order to determine their unique pattern. The powder samples were compacted in a square aluminum sample container (40 mm) with a one-millimeter deep rectangular hole (20 mm 15 mm) and pushed against an optically smooth glass panel. In the same plane as the top surface of the sample, the sample holder's label was affixed to the plane. Following that step, the sample holder was installed into the diffractometer.

2.8. Vibrating sample magnetometer (VSM)

An instrument called a vibrating sample magnetometer was used to examine the magnetic characteristics of the Ag NPs (EV-9 Micro Sense, German). In this investigation, the first thing that needed to be done was to build a vibrating mechanism that was capable of vibrating the sample at an amplitude that was both quantifiable and tunable. The last phase consisted of the magnetic field used for perturbations, detected by the detecting coils.

3. Results and discussion

3.1. X-ray Diffraction (XRD) analysis

The crystalline nature of the green synthesized AgNPs was confirmed using the XRD technique, and the corresponding XRD patterns of the green synthesized Ag NPs for 20 mM (a); 50 mM (b); and 100 mM (c) are shown in Fig.2. The diffraction peaks of synthesized Ag NPs for 20 mM solution (a) were obtained at the 2θ values of 38.19°, 44.42°, and 64.49° corresponded to the planes (111), (200), and (220), respectively. For synthesized Ag NPs for 50 mM (b), diffraction peaks were found at the 2θ values of 38.19°, 44.42°, and 64.61°, which corresponded to the planes (111), (200), (220), respectively. Similar diffraction peaks were observed for synthesized silver nanoparticles from 100mM AgNO3 solution indicated in Figure 2 and denoted by (c) where the 2θ values were 38.30°, 44.52°, 64.61°. We also investigated the corresponding plane of the 2θ value and likely to the plane (111), (200), and (220), respectively. For every set of 2θ values and plane direction, this is understandable that the prepared AgNPs are face-centered cubic [20]. In addition, the unspecified peaks may be concomitant with the organic compounds which originate from the *Mangiferaindica* leaf extract and act as capping agents that stabilize the Ag NPs [20]. Scherrer's formula determined the average crystallite size of the ready samples (a, b, c) from the most substantial peak. The calculated crystallite size was about 35.43 nm, 14.89 nm, and 61.90 nm. Moreover, the smaller the particle sizes are because the particles are encapsulated at the time of nucleation, hindering the aggregation and reducing the particle size [21]. Generally, increasing the concentration of the precursor, the rate of nucleation rises with an increase in particle size [21].

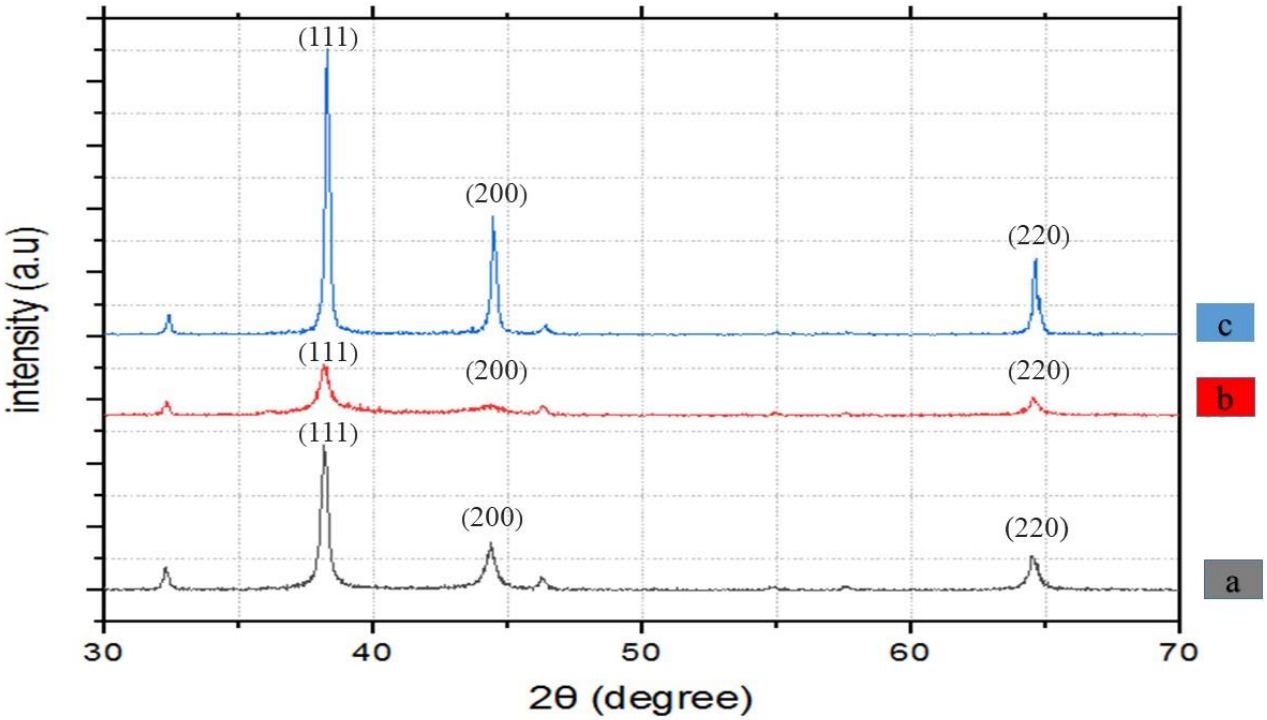

Figure 2: (a) XRD patterns of the green synthesized Ag NPs for 20 mM; (b)XRD patterns of the green synthesized Ag NPs for 50 mM; (c) XRD patterns of the green synthesized Ag NPs for 100 mM.

3.2. Thermo-gravimetric Analysis (TGA)

In order to consider the consequence that temperature has on 20mM, 50mM, and 100mM solution-mediated Ag NPs, Thermo-gravimetric Analysis (TGA) was carried out between 25°C and 800 °C, and the corresponding data are shown in Figure 3 (a, b, and c curves, respectively). The initial weight loss was detected up to 159.97 °C (1.22%) in (a), up to 173 °C (2.99%) in (b), and up to146.58 °C (5.88%) in (c), which may be attributed to the release of water molecules occupied on the surface of Ag NPs [22].

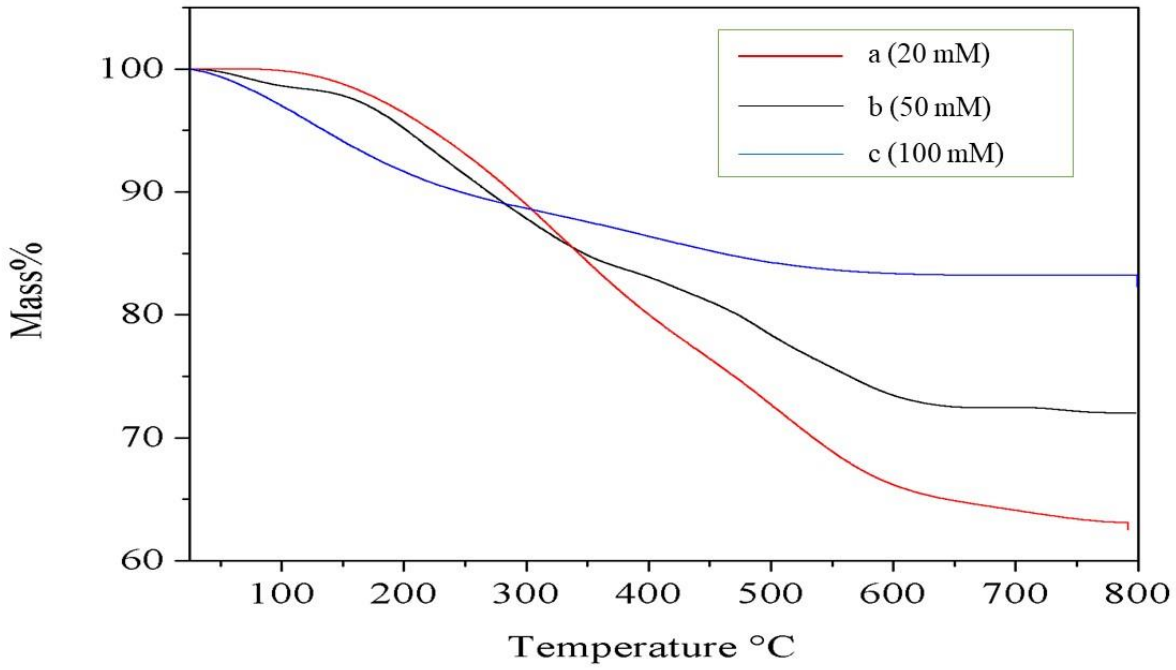

Figure 3: TGA plot for as synthesized silver nanoparticles Ag NPs using 20mM $AgNO_3$ (a), 50 mM $AgNO_3$ (b) and 100mM $AgNO_3$ (c) solution.

The second weight loss was obtained up to 705.30 °C (35.96%), 604.36°C (26.7%), and 533.43°C (16.63%) for the (a), (b), and (c) TGA curve respectively that might be due to the ejection of organic compounds attached on the surface of Ag NPs acted as capping agents. Similar studies were reported by earlier workers [22]. The curve was not remaining steady among the whole range, but it started to become constant from just before 800°C.

3.3 Fourier Transform Infrared (FT-IR) spectra analysis

The FT-IR spectra of the sample of *Mangifera indica* (Mango) leaf powder and synthesized Ag NPs were documented by an FTIR spectrometer in the 4000 – 400 cm^{-1} and shown in Figure 4. In the figure, there are four curves as a, b, and c FTIR Spectra for Ag NPs using 20 mM $AgNO_3$, 50 mM $AgNO_3$, and 100 mM $AgNO_3$ solution respectively. Another Spectrum is pure Mango Leaf powder which is denoted as d.To determine the potential causes, FT-IR analysis was performed on the biomolecules that were found to be responsible for the degradation of the Ag+ ions as well as the capping agents that were shown to be responsible for the stability of the Ag NPs. Fig. 4 (curved d) represents the FT-IR spectrum of the plain *Mangifera indica* leaf (mango leaf) extract powder. The peaks were obtained at 478.42, 661.52,787.87, 1068.56, 1313.52, 1431.18, 1635.54, 2856.58,

2922.16, 3419.79, 3707.18, 3772.76 cm^{-1} which agreed well with the reported values [23]. The matching organic functional groups for peak standards were might be 478.42 cm^{-1} for C-X (Alkyl halide), 661.52 cm^{-1} for C-Cl (Alkyl chloride), 1068.56 cm^{-1} for O-H (Alcohol) or C-F (Alkyl fluoride), 1313.52 cm^{-1} for different sorts of amines group (N-H), 1431.18 $cm^{-1}$for -C-H (Alkane) or C=C (Aromatic), 1635.54 cm^{-1} for C=C (Alkene) or C=O (Carbonyl), 2856.58 cm^{-1}, and 2922.16 cm^{-1} for alkanes [24]. The terpenoids also compact silver ions and oxidized to carboxyl groups, thus, consequential in a band at 1635.54 cm^{-1}. The peak corresponding to the amine band at 1313.52 cm^{-1} has extended and specifies the protein's coating of the silver nanoparticles [25]. It is well known that proteins have the capability to attribute to Ag NPs through free amine group remainders [26]. A comparable mechanism could be functioning in the contemporary case where proteins extracted from the mango leaf capped the Ag NPs [26]. Analyzing Figure 4 (curve a), the obtained peaks correspond to 472.56 cm^{-1} for (Alkyl Halide), 1072.42 cm^{-1} for (Alcohol) or C-N (Amine), 1622.13 cm^{-1} for C=C(Alkene), 2860.43 cm^{-1}, and 2922.16 cm^{-1} for alkanes C-H, 3442.94 cm^{-1} for O-H (Alcohol) or N-H (Amine), 3701.40 cm^{-1}, and 3770.84 cm^{-1} for O-H (Alcohol) [27]. We can pay no consideration to the possibility that approximately other bioorganic compounds can be present in solution and contribute to reducing silver ions and stabilizing the nanoparticles thus shaped by surface capping. At the moment, work is being done to separate the various bioorganic fractions found in the broth made from mango leaves and examine each one separately for their ability to reduce the number of silver ions and bond with the nanoparticles. In Figure 4 (curve b), it was apparent that the leaf extract reconciled Ag NPs and the found peaks are matched to 484.13 cm^{-1} for (Alkyl Halide), 1068.56 for (Alcohol) or C-N (Amine), 1633.71 cm^{-1} for C=C(Alkene), 2856.58 cm^{-1}, and 2924.09cm^{-1} for alkanes C-H, 3452.22cm^{-1} for O-H (Alcohol) or N-H (Amine), 3689.83cm^{-1}, and 3780.48 cm^{-1} for O-H (Alcohol) [27]. Among them, a group of organic compounds can be present in the solution and contribute to the elimination of silver. The consolidation of nanoparticles was both successful and worked like a capping agent. Similarly, Fig. 4 (curve c) confirmed picks at 480.28 cm^{-1} for (Alkyl Halide), 1099.43 for (Alcohol) or C-N (Amine), 1635.64 cm^{-1} for C=C(Alkene), 2873.94 cm^{-1} for alkanes C-H, 3442.94 cm^{-1} for O-H (Alcohol) or N-H (Amine), 3697.54 cm^{-1}, and 3766.98 cm^{-1} for O-H (Alcohol) respectively [28]. All the picks were organic functional groups, and these organic groups have a huge influence on the reducing and capping properties of nanoparticles.

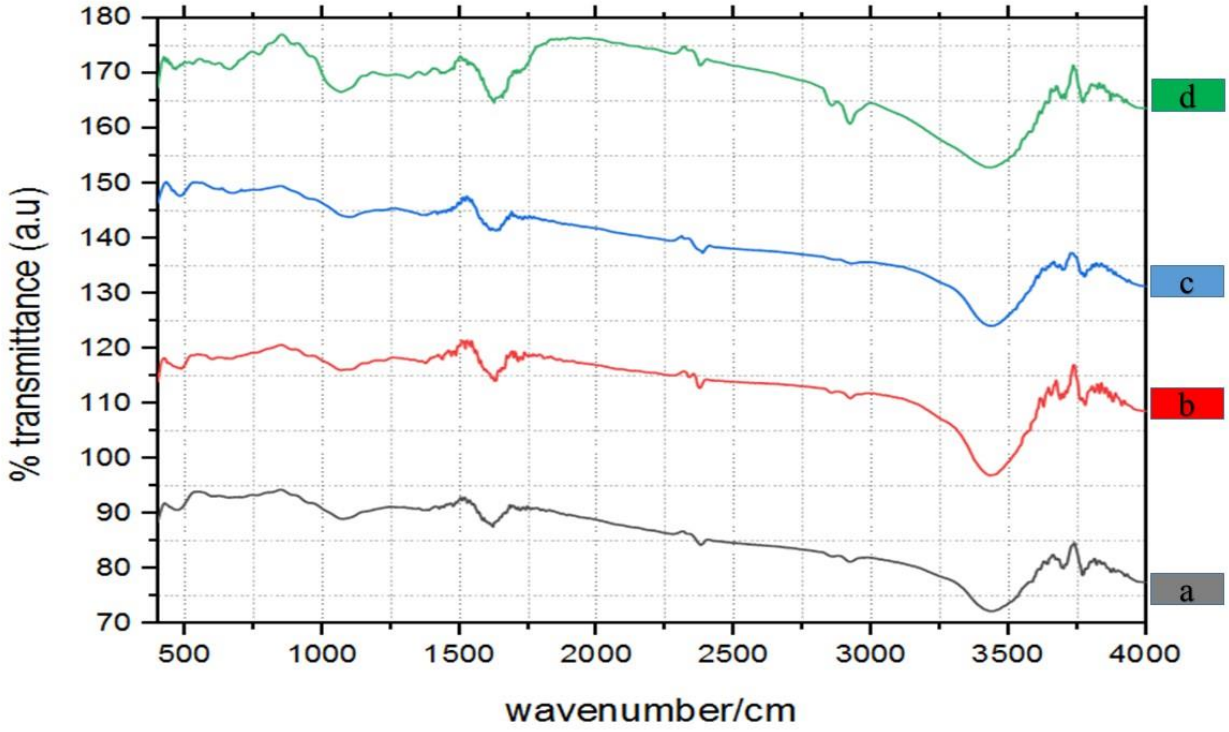

Figure 4: FT-IR spectra of *Mangifera indica* leaf extract arbitrated synthesized Ag NPs for (a) 20 mM $AgNO_3$ solution, (b) 50 mM $AgNO_3$ solution. (c) 100 mM $AgNO_3$ solution and (d) *Mangifera indica* leaf powder.

Another interesting finding is that the above FT-IR spectra show almost similar bands for the synthesized Ag NPs. However, the peak intensities were shown to be different. The variation of the peak intensities was due to the encapsulation of the bio-molecules coming from the mango leaf extract during Ag NPs synthesis.

3.4 Energy Dispersive X-ray (EDX) spectroscopy analysis

Elemental investigation of the produced Ag NPs was performed using EDX spectra analysis shown in Figure 5 (a) EDX image (for 20 mM $AgNO_3$ solution), (b) EDX image (for 50 mM $AgNO_3$ solution), (c) EDX image (for 100 mM $AgNO_3$ solution) showing the presence of Ag NPs and bioorganic components coming from *Mangifera indica* leaf extract**.** The EDX profile exhibited clear indications of the presence of silver atoms.

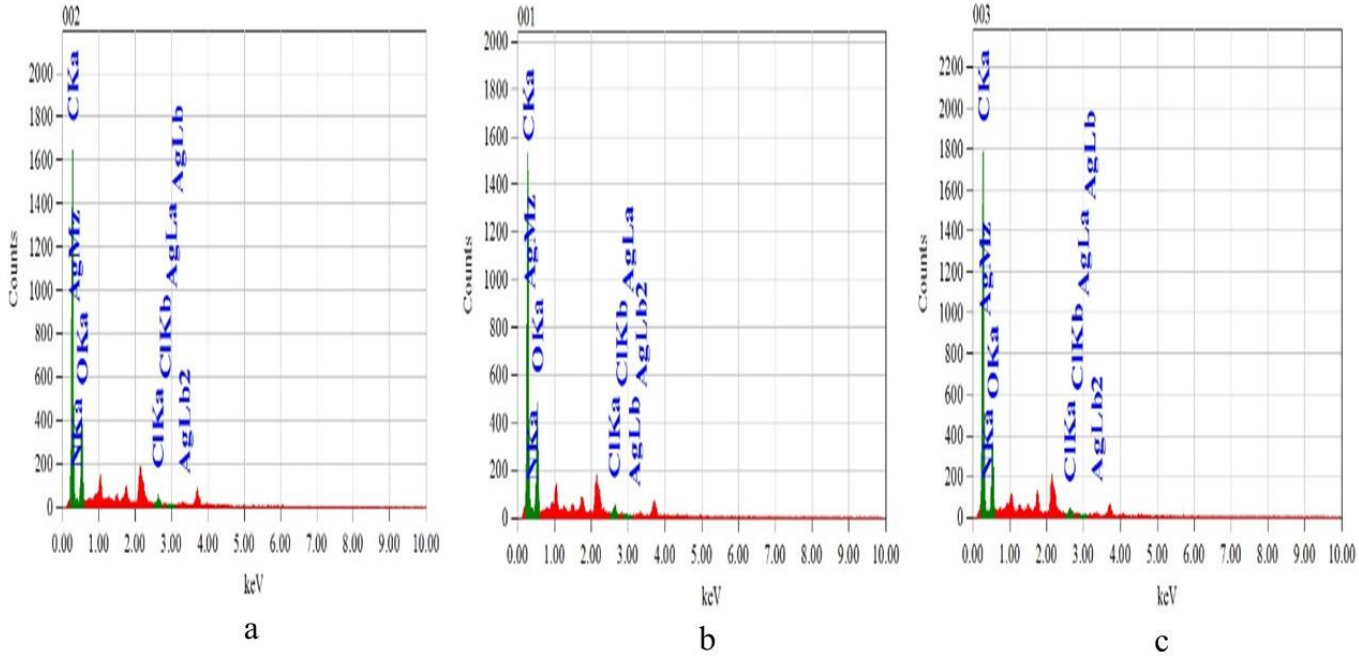

Figure 5: (a) EDX image (for 20 mM $AgNO_3$ solution), (b) EDX image (for 50 mM $AgNO_3$ solution), (c) EDX image (for 100 mM $AgNO_3$ solution) showing the presence of Ag NPs and bioorganic components coming from *Mangifera indica* leaf extract.

The peak of the strong signal was almost identical. The fact that it was located at an accumulation of 3.25 keV in the EDX spectra, which was characteristic of the absorption of silver nanocrystallites [29], demonstrated the existence of Ag NPs. It's interesting to note that additional elements including carbon, chlorine, nitrogen and oxygen were found as well. C and O are most likely connected with the organic compounds from the extract that were absorbed on the surface of the Ag NPs [29]. These organic compounds play an important role in the reduction and stability of Ag NPs. Cl was found in the solution that was made from the leaf extract.

3.5 Scanning Electron Microscopy (SEM) analysis

The surface morphology of the synthesized Ag NPs (for 20 mM $AgNO_3$ solution) was monitored using Scanning Electron Microscopy (SEM) technique and shown in Figure 6 (a, b, c, d). The synthesized Ag NPs (for 50 mM $AgNO_3$ solution) presented in Figure 6 (e, f, g, h) and similarly synthesized Ag NPs (for 100 mM $AgNO_3$ solution) illustrated in Figure 6 (i, j, k, l). The SEM images of Ag NPs established that the synthesized Ag NPs are uniformly circulated with minimal accumulation for the above three concentrations of The Ag NPs obtained were with contracted size dissemination from 10 to 100 nm approximately. In every high-resolution SEM image, the particle size and distribution were apparent. The particle size and their shape were almost analogous for all

concentrations. Some bulky particles are seen as probably resulting from the accumulation of small ones [30]. The large particle may be removed through heat treatment. A similar observation was also found in different works [30].

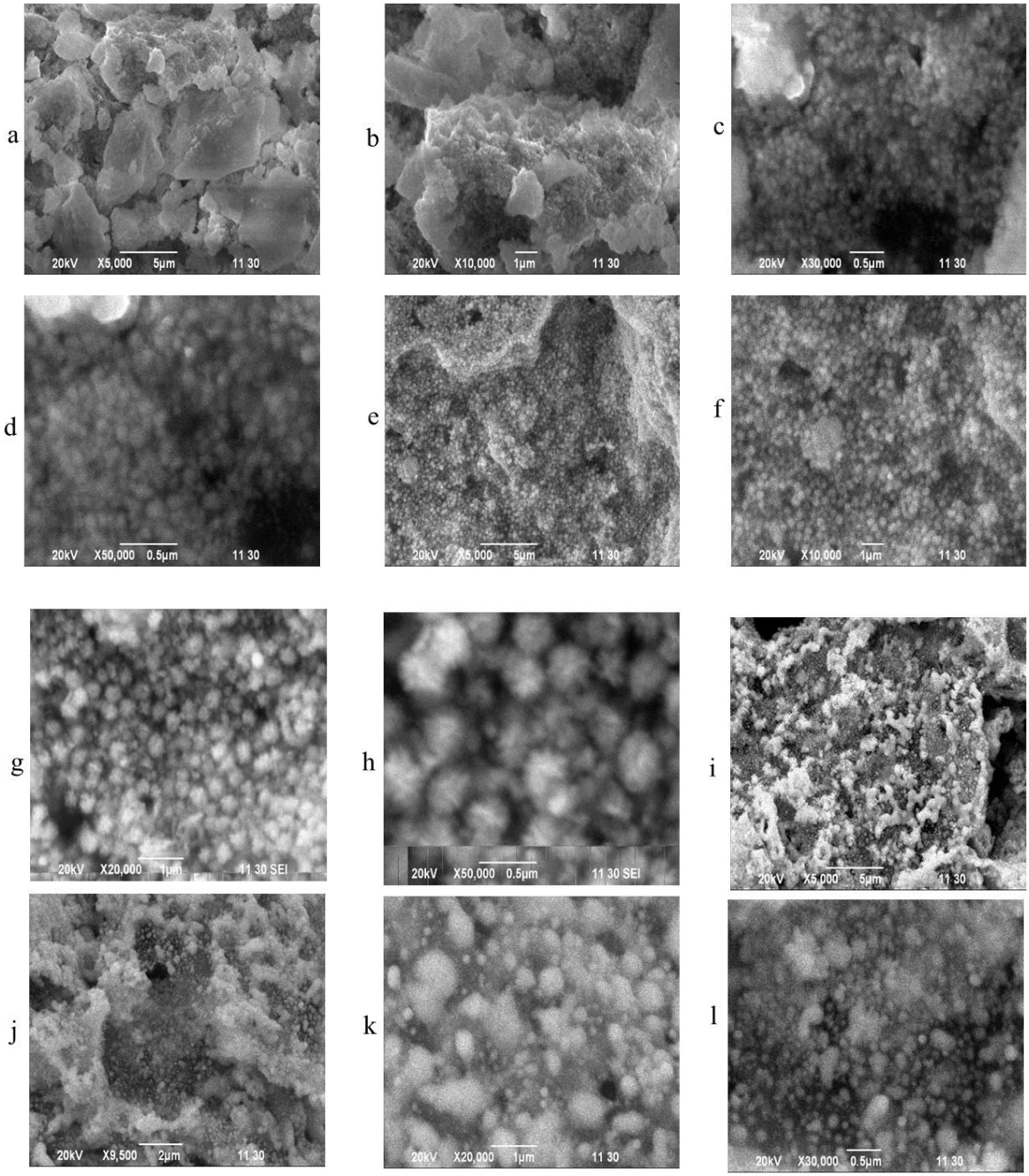

Figure 6: SEM micrographs of several regulations (a, b, c, d), SEM micrographs of the biosynthesized Ag NPs synthesized using 20 mM $AgNO_3$ solution. Fig. (e, f, g, h), SEM micrographs of the biosynthesized Ag NPs synthesized using 50 mM $AgNO_3$ solution. Fig (I, j, k, l), SEM micrographs of the biosynthesized Ag NPs synthesized using 100 mM $AgNO_3$ solution.

3.6 Magnetic property analysis

The magnetic property of synthesized Ag NPs was examined using Vibrating Sample Magnetometer (VSM) analysis for 20 mM, 50 mM, and 100 mM $AgNO_3$ solution mediated Ag NPs. The corresponding hysteresis loop is shown in Figure 7 (a, b, c). From the hysteresis loops of VSM analysis, it is found that the synthesized Ag NPs showed weak ferromagnetic nature at room temperature. The calculated saturation magnetization from three loops were ranged from 0.081 emu g^{-1} to 0.116 emu g^{-1}. On the other hand the value of coercivity between 125 Oe and 161 Oe. Both of this result indicated clearly weak ferromagnetic nature of synthesize Ag NPs. Ferromagnetic behavior of Ag NPs was also reported earlier [31]. The critical importance of size in defining nanomaterials electrical, chemical, optical, and magnetic characteristics is well recognized [32]. A noteworthy new finding is the ferromagnetism of nanoparticles of metal oxides and other inorganic materials, which are normally diamagnetic in the bulk form [32]. In particular, there are the magnetic characteristics of nanoparticles of metals such as Au and Ag [33]. We discovered magnetism in roughly 3 nm Au and Ag NPs shielded by polyvinyl pyrrolidone (PVP) with unusually significant magnetic moments of around 20 spins per particle. Since then, a few additional writers have found magnetism in Au nanoparticles, however, the origin of ferromagnetism in Au nanoparticles has remained somewhat unexplained [34]. In most published investigations, the Au nanoparticles were coated with capping agents such as thiols and amines [35]. Researchers limited reported that gold nanoparticles coated with weakly interacting chemicals like tetra alkylammonium bromides are diamagnetic. However, those shielded by strongly interacting thiols are ferromagnetic because of the 5d localized holes formed during Au–S charge transfer [36]. The genesis of orbital magnetism coming from spin-orbit coupling owing to this charge transfer has been studied [36]. However, they reported more effective ferromagnetic spin coupling in gold nanoparticles poorly protected with polyacrylonitrile, poly (allylamine hydrochloride), and PVP [37]. They ascribe the particle-size-dependent ferromagnetic character of the surface Au atoms to the so-called Fermi hole effect [38]. From the documented ferromagnetic characteristics of Au NPs, it may be claimed that the ferromagnetic behavior of our green produced Ag NPS is owing to the nano-sized dimension, amine and thiol groups being present on the surface of the silver nanoparticles (Ag NPs) (Ag NPs). It is also agreed with the EDS and FT-IR studies. Similar findings were also obtained in a prior study.

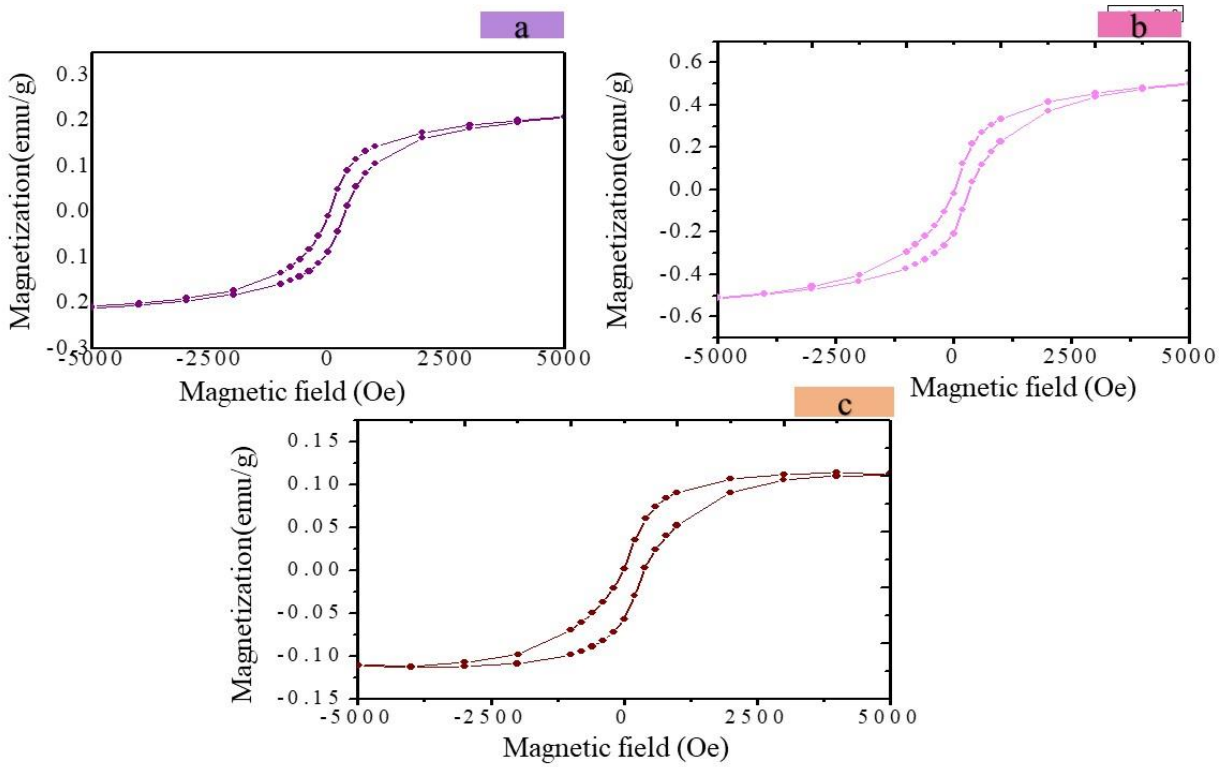

Figure 7: Magnetization curve of synthesized silver nanoparticles synthesized using *Mangifera indica* leaf (mango leaf) extract (a) for 20 mM $AgNO_3$solution. (b) for 50 mM $AgNO_3$solution. (c) for 100 mM $AgNO_3$solution.

4. Conclusions

The present investigation concluded that the green synthesis of Ag NPs, using *Mangifera indica* leaf extract as a reducing and capping agent, has advantages such as ease of availability, simplicity, and eco-friendliness. This permits for the progression to be scaled up and preserves its economic viability. Different biomolecules in the leaf extract confirmed by the FT-IR analysis acted as reducing agents. The XRD peaks are ascribed to the FCC structure of silver. The X-ray Diffraction (XRD) technique showed from the most substantial peak using Scherrer's formula the crystalline size of Ag NPs for 20 mM $AgNO_3$) as 35.43 nm, Ag NPs (for 50 mM $AgNO_3$) at 14.89 nm, and Ag NPS (for 100 mM$AgNO_3$) as 61.90 nm. The EDX investigation also long-established the formation of Ag NPs and the attendance of the elements of the coating agents coming from the leaf extract. TGA exhibited the first weight loss that occurs for removing attached water molecules from the surface of Ag NPs as well as the second loss for eliminating organic compounds. In the temperature region, the surface morphology, and particle dimension were examined by Scanning Electron Microscopy (SEM) analysis and found to be between 10-100 nm for all three concentrations of AgNO3. From VSM analysis, we know that bulk silver is nonmagnetic, but the biosynthesized Ag NPs are weak ferromagnetic. From this analysis, we get a green synthesis that is energy-efficient, cost-effective;

protect human health, and eco-friendly. This eco-friendly method has the potential to be a competitive alternative to the conventional physical and chemical approaches used to synthesize silver nanoparticles. As a result, it has the potential to be used in biomedical applications and will shortly play an essential role in optoelectronics and medical devices.

Conflicts of interest

The authors declare no conflict of interest.

Acknowledgements

The authors would like to acknowledge Materials Science Division, Atomic Energy Centre Dhaka; Department of Physics, University of Dhaka; and Department of Glass and Ceramic Engineering, Bangladesh University of Engineering and Technology for their assistance for the characterization.

References

1. S. Liu, S. A. Qamar, M. Qamar, K. Basharat, M. Bilal, Engineered nanocellulose-based hydrogels for smart drug delivery applications. *International Journal of Biological Macromolecules*. **181**, 275-290 (2021)

2. B. Han, L. Zhang, S. Zeng, S. Dong, X. Yu, R. Yang, J. Ou, Nano-core effect in nano-engineered cementitious composites. *Applied Science and Manufacturing*. **95,** 100-109 **(**2017).

3. L. Sun, R. Wei, J. Feng, H. Zhang, Tailored lanthanide-doped up conversion nanoparticles and their promising bio-application prospects. *Coordination Chemistry Reviews*. **364**, 10-32 (2018)

4.V. K. VG, A. A. Prem, Green synthesis and characterization of iron oxide nanoparticles using Phyllanthus niruri extract. *Oriental Journal of Chemistry*. **34**, 2583-2593 (2018)

5. E. Abbasi, M. Milani, S. Aval, M. Kouhi, , A. Akbarzadeh, H. Nikasa, P. Joo, S. W. Hanifehpour, Y. Nejati-Koshki, M. Samiei, Silver nanoparticles: synthesis methods, bio-applications and properties. *Critical reviews in microbiology*. **42,** 173-180 (2016)

6. S. Gul, S. B. Khan, I. U. Rehman, M.A. Khan, M. I. Khan, A comprehensive review of magnetic nanomaterials modern day theranostics. *Frontiers in Materials*. **6,** 179-195 (2019)

7. M. Elangovan, G. Muju, P. Anantharaman, Biosynthesis of Silver Nanoparticles from Platymonas sp. and Its Antibacterial Activity Against Biofouling Causing Bacterial Strains. *Journal of Biologically Active Products from Nature*. **9**, 269-277 (2019)

8. A. K. Deshmukh, S. S. Gaikwad, D. N. Pansare, R. N. Shelke,C. H. Gill, Synthesis of some benzothiazole derivatives by using zinc oxide nanoparticles. *Journal of Current Pharma Research*. **9,** 2927-2934 (2019)

9. K. Anandalakshmi, J. Venugobal, V. Ramasamy, Characterization of silver nanoparticles by green synthesis method using Pedalium murex leaf extract and their antibacterial activity. *Applied nanoscience*. **6,** 399-408 (2016)

10. S.S.D. Kumar, N.K. Rajendran, N.N. Houreld, H. Abrahamse, Recent advances on silver nanoparticle and biopolymer-based biomaterials for wound healing applications. *International journal of biological macromolecules*. **115,** 165-175 (2018)

11. A. Haider, I. K. Kang, Preparation of silver nanoparticles and their industrial and biomedical applications: a comprehensive review. *Advances in materials science and engineering*. **7,** 235-245 (2015).

12. P. Khandel, R. K. Yadaw, D. K. Soni, L. Kanwar, S. K. Shahi, Biogenesis of metal nanoparticles and their pharmacological applications: present status and application prospects. *Journal of Nanostructure in Chemistry*. **8,** 217-254 (2018).

13. M. Z. H. Khan, F. K. Tareq, M. A. Hossen, M. N. A. M. Roki, Green synthesis and characterization of silver nanoparticles using *Coriandrum sativum* leaf extract. *Journal of Engineering Science and Technology*. **13,** 158-166 (2018).

14. D. A. Selvan, D. Mahendiran, R.S. Kumar, A. K. Rahiman, Garlic, green tea and turmeric extracts-mediated green synthesis of silver nanoparticles: Phytochemical, antioxidant and in vitro cytotoxicity studies. *Journal of Photochemistry and Photobiology B: Biology*. **180,** 243-252 (2018).

15. P. Chandra, R. Singh, P. K. Arora, Microbial lipases and their industrial applications: a comprehensive review. *Microbial Cell Factories*. **19,** 1-42 (2020).

16. A. Singh, S. M. Prasad, Nanotechnology and its role in agro-ecosystem: a strategic perspective. *International Journal of Environmental Science and Technology*. **14,** 2277-2300 (2017).

17. S. O. Aisida, K. Ugwu, A. C. Nwanya, A. K. H. Bashir, N. U. Nwankwo, I. Ahmed,F. I.Ezema, Biosynthesis of silver oxide nanoparticles using leave extract of Telfairia Occidentalis and its antibacterial activity. *Materials Today*. **36**, 208-2013 (2021).

18. B. Mirza, C. R. Croley, M. Ahmad, J. Pumarol, N. Das, G. Sethi, A. Bishayee, Mango (*Mangifera indica* L.): a magnificent plant with cancer preventive and anticancer therapeutic potential. *Critical Reviews in Food Science and Nutrition*, **61,** 1-27 (2021).

19. P. Suchomel, L. Kvitek, R. Prucek, A. Panacek, A. Halder, S. Vajda, R. Zboril, Simple size-controlled synthesis of Au nanoparticles and their size-dependent catalytic activity. Sci. Rep. **8,** 1-11 (2018).

20. B. Malaikozhundan, S. Vijayakumar, B. Vaseeharan, A. A. Jenifer, P. Chitra, N. M. Prabhu, E. Kannapiran, Two potential uses for silver nanoparticles coated with Solanum nigrum unripe fruit extract: biofilm inhibition and photodegradation of dye effluent. *Microbial pathogenesis*. **111**, 316-324 (2017).

21. J. H. Jo, P. Singh, Y. J. Kim, C. Wang, R. Mathiyalagan, C. G. Jin, D. C. Yang, Pseudomonas deceptionensis DC5-mediated synthesis of extracellular silver nanoparticles. *Artificial cells, nanomedicine, and biotechnology*. **44**, 1576-1581 (2016)

22. K. Afshinnia, B. Marrone, M. Baalousha, Potential impact of natural organic ligands on the colloidal stability of silver nanoparticles. *Science of The Total Environment*. **625,** 518-1526 (2018)

23. A. U. Khan, Q. Yuan, Z. U. H. Khan, A. Ahmad, F. U. Khan, K. Tahir, M. Shakeel, S. Ullah, An eco-benign synthesis of Ag NPs using aqueous extract of Longan fruit peel: Antiproliferative response against human breast cancer cell line MCF-7, antioxidant and photocatalytic deprivation of methylene blue. *Journal of Photochemistry and Photobiology B: Biology*. **183**, 367-373 (2018).

24. B. Kumar, K. Smita, R. Seqqat, K. Benalcazar, M. Grijalva, L. Cumbal, In vitro evaluation of silver nanoparticles cytotoxicity on Hepatic cancer (Hep-G2) cell line and their antioxidant activity: Green approach for fabrication and application. *Journal of Photochemistry and Photobiology B: Biology*. **159**, 8-13 (2016).

25. A. Gul, A. Shaheen, I. Ahmad, B. Khattak, M. Ahmad, R. Ullah, A. Bari, S. S. Ali, A. Alobaid, M. M. Asmari, H. M. Mahmood, Green synthesis, characterization, enzyme inhibition, antimicrobial potential, and cytotoxic activity of plant mediated silver nanoparticle using Ricinus communis leaf and root extracts. *Biomolecules*. **11**, 206-213 (2021)

26. K. Priya, M. Vijayakumar, B. Janani, Chitosan-mediated synthesis of biogenic silver nanoparticles (Ag NPs), nanoparticle characterization and in vitro assessment of anticancer activity in human hepatocellular carcinoma HepG2 cells. *International journal of biological macromolecules*. **149,** 844-852 (2020).

27. N. Kizildag, N. Ucar, Investigation of the properties of PAN/f-MWCNTs/Ag NPs composite nanofibers. *Journal of Industrial Textiles*. **47**, 149-172 (2017).

28. U. Muthukumaran, M. Govindarajan, M. Rajeswary, S. Hoti, Synthesis and characterization of silver nanoparticles using Gmelina asiatica leaf extract against filariasis, dengue, and malaria vector mosquitoes. *Parasitology research*. **114**, 1817-1827 (2015)

29. G. Muthusamy, S. Thangasamy, M. Raja, S. Chinnappan, S. Kandasamy, Biosynthesis of silver nanoparticles from Spirulina microalgae and its antibacterial activity. *Environmental Science and Pollution Research*. **24**, 19459-19464 (2017).

30. A. Rautela, J. Rani, Green synthesis of silver nanoparticles from Tectona grandis seeds extract: characterization and mechanism of antimicrobial action on different microorganisms. *Journal of Analytical Science and Technology*. **10**, 1-10 (2019).

31. P. Nehla, C. Ulrich, R. S. Dhaka, Investigation of the structural, electronic, transport and magnetic properties of Co2FeGa Heusler alloy nanoparticles. *Journal of Alloys and Compounds*. **776**, 379-386 (2019)

32. S. Bard, F. Schönl, M. Demleitner, V. Altstädt, Copper and nickel coating of carbon fiber for thermally and electrically conductive fiber reinforced composites. *Polymers*. **11**, 823-832 (2019)

33. I. Majeed, M. A. Nadeem, M. Al-Oufi, M. A. Nadeem, G. I. N. Waterhouse, A. Badshah, J.B. Metson, H. Idriss, On the role of metal particle size and surface coverage for photo-catalytic hydrogen production: A case study of the Au/CdS system. *Applied Catalysis B: Applied Catalysis B. Environmental*. **182**, 266-276 (2016).

34. R. Sato, S. Ishikawa, H. Sato, and T. Sato, Magnetic order of Au nanoparticle with clean surface. *Journal of Magnetism and Magnetic Materials*. **393**, 209-2012 (2015).

35. B. Steinfeld, J. Scott, G. Vilander, L. Marx, M. Quirk, J. Lindberg, K. Koerner, The role of lean process improvement in implementation of evidence-based practices in behavioral health care. *The Journal of*

Behavioral Health Services & Research. **42**, 504-518 (2015).

36. S. Bag, S. Bhattacharya, D. Dinda, M. V. Jyothirmai, R. Thapa, S. K. Saha, Induced ferromagnetism and metal-insulator transition due to a charge transfer effect in silver nanoparticle decorated MoS2. *Physical Review B*. **98**, 014109-0141115 (2018).

37. X. Li, A. Sotto, J. Li, B. V. Bruggen, Progress and perspectives for synthesis of sustainable antifouling composite membranes containing in situ generated nanoparticles. *Journal of Membrane Science*. **524**, 502-528 (2017).

38. K. Dolui, B. K. Nikolić, Spin-orbit-proximitized ferromagnetic metal by monolayer transition metal dichalcogenide: Atlas of spectral functions, spin textures, and spin-orbit torques in Co/MoSe 2, Co/WSe 2, and Co/TaSe 2 heterostructures. *Physical Review Materials*. **4,** 104007-1040030 (2020).